

High Resolution 3D Multi-slab Multi-shot Spin Echo Diffusion-Weighted Imaging

A. T. Van¹, D. C. Karampinos², and B. P. Sutton^{3,4}

¹Electrical and Computer Engineering, University of Illinois, Urbana, IL, United States, ²Radiology and Biomedical Imaging, University of California, San Francisco, CA, United States, ³Bioengineering, University of Illinois, Urbana, IL, United States, ⁴Beckman Institute, University of Illinois, Urbana, IL, United States

Introduction: The need to detect small brain lesions and to reduce partial volume effects in fiber tractography has made high resolution isotropic 3D diffusion-weighted imaging (DWI) a research focus in diffusion acquisition methodology [1-4]. To achieve reasonable scan time, most of the proposed 3D DWI methods used steady-state free precession (SSFP) acquisition [1-3] which has a complicated diffusion-weighted signal model that requires separate T1 and T2 measurements. 3D spin-echo DWI can be described by the standard Stejskal-Tanner signal model, but it is limited by prolonged acquisition times, especially when combined with cardiac gating. In this work, we propose to use a **multi-slab multi-shot DW spin echo (SE)** sequence to achieve high resolution 3D DW imaging with whole brain coverage within a reasonable scan time. 3D multi-slab acquisition is proposed to reduce the total scan time relative to single-slab 3D spin-echo DWI acquisition without a loss in SNR efficiency. Motion-induced phase errors resulting from multi-shot acquisition are corrected based on 3D navigators using the KICT algorithm proposed in [5, 6].

Method: 3D multi-slab acquisition: 3D multi-slab acquisition has been used previously in magnetic resonance angiography [7]. In 3D multi-slab acquisition the whole 3D imaging volume is divided into smaller 3D imaging volumes called slabs. Since each of the slabs in a 3D multi-slab acquisition is excited and imaged independently, the slabs can be interleaved to achieve shorter total acquisition time as compared to the conventional, single slab 3D imaging. Shorter acquisition times make the 3D multi-slab acquisition more immune to gross motion within a volume and across volumes, giving high quality DW images and diffusion metric maps. Another advantage of multi-slab acquisition is that when cardiac-gated acquisition is used, multi-slab acquisition allows different parts of the brain to be acquired during different parts of the cardiac cycles giving better cancellation of pulsation effects. This cardiac-gated strategy has been proposed elsewhere [8] for 2D DWI.

Disadvantages of 3D multi-slab acquisition include boundary artifacts and possible loss of signal-to-noise ratio (SNR) as compared to equivalent single slab 3D acquisitions. Boundary artifact of multi-slab acquisition can be reduced by overlapping adjacent slabs, interleaving odd and even slabs (Figure 1), and discarding some boundary slices of the 3D reconstructed slab images.

3D trajectory and 3D navigator: The 3D trajectory used in the current study was a stack of multishot

constant density spirals. For motion-induced phase error correction, a stack of low resolution single shot constant density spirals was used as the navigator. Navigator data were acquired after every data acquisition by adding a second refocusing pulse to the spin echo sequence [6].

Phase error correction and image reconstruction: Cardiac-gating was used to minimize non-linear motion-induced phase errors. Linear motion-induced phase errors were estimated from the navigator data by subtracting the phase of the diffusion encoded navigator images with the phase of the $b = 0$ navigator images. Slopes and offsets of the linear phase errors were then estimated with least squares fitting and used to correct the k -space of the data [5, 6]. Corrected k -space data were then reconstructed using NUFFT [9] with the quadratic penalized weighted least squares (QPWLS) iterative algorithm. For the navigating data, a faster reconstruction including gridding in-plane and 1D FFT through-plane was used [6].

Results: SNR analysis: Let SNR_{3D} and SNR_{2D} be the SNRs of 3D (Cartesian sampling in the third dimension) and 2D interleaved spin echo acquisitions, respectively. For cardiac-gated acquisition with at most n_{exc} number of excitations per cardiac cycle, the ratio of SNR between 3D multi-slab and 3D single slab acquisitions is given in Equation (1) (assuming similar diffusion encoding, similar readout duration). For 3D single slab acquisition, multiple excitations within a cardiac cycle are not employed due to the resulting short TR and severe SNR degradation. In Equations (1), n_{slab} is the number of slabs in a 3D multi-slab acquisition, N_{p2} is the number of the third dimension encoding steps, TE is the echo time of the sequence, and $T1$, $T2$ are the relaxation times. For the case where $n_{slab} = 6$, $n_{exc} = 3$, $N_{p2} = 96$, $RR = 1$ s, $TE = 68$ ms, $T1 = 1081$ ms, $T2 = 69$ ms, $SNR_{3D}(\text{multi}) = 0.59$ $SNR_{3D}(\text{single})$. However, the total acquisition time of 3D multi-slab, is **3 times shorter** than that of 3D single slab acquisition. If we define as SNR efficiency the ratio of SNR over the square root of the total scan time, 3D multi-slab acquisition has then the same SNR efficiency (since $0.59 \times 3^{1/2} = 1.02$) as the 3D single slab acquisition, but enables three times shorter scan time. Similar comparison is done for 3D multi-slab and equivalent interleaved 2D acquisition giving $SNR_{3D}(\text{multi}) = 3.33$ SNR_{2D} with the **same total acquisition time**.

In vivo data were acquired using Siemens 3 T Trio scanner with a 12-channel head coil on a healthy male subject in accordance with the institutional review board. The obtained resolution was $1.88 \times 1.88 \times 1.88$ mm³ with full brain coverage. Other imaging parameters were: TE1 = 68 ms (for data), TE2 = 120 ms (for the navigator), $b = 1000$ s/mm², 3-shot constant density spiral in-plane trajectory with readout duration of 20.08 ms, 6 slabs with 16 Cartesian encoding steps per slab, overlapping factor of 25% of slab thickness. The acquisition was cardiac-gated with 3 slabs per R-R interval, resulting in an effective TR of 2 R-R intervals. If slabs were numbered from 1 to 6 starting from the lower part of the brain, slab acquisition order was [1 3 5; 2 4 6]. The k -space FOV of the navigator data were $10 \times 10 \times 10$ (1/FOV). The total acquisition time for one 3D volume, one direction is **96 s** on subjects with an R-R interval of 1s. Figure 2 shows the obtained diffusion-weighted image without (a) and with (b) motion-induced phase error correction, respectively. The correction algorithm effectively removed the artifacts and restored signal in the uncorrected images giving high quality DW images. Slab boundary artifacts are still visible although not severe. Furthermore, since the slab boundary artifacts are consistent through all images, the resulting diffusion metric maps will not be significantly affected as shown in Figure 3. FA maps were obtained with 13 diffusion encoding directions.

Discussion and Conclusion: We have proposed a novel 3D high resolution DWSE acquisition strategy for whole brain coverage. *In vivo* high quality $1.88 \times 1.88 \times 1.88$ mm³ resolution DW images and FA maps with whole brain coverage were obtained within reasonable scan time. With appropriate slab acquisition order and cardiac gating, the proposed technique is fairly immune to pulsation. Compared with other SSFP based techniques [1-3], our acquisition scheme can achieve similar resolution within similar total acquisition time while using the standard Stejskal-Tanner signal model. Compared to fast spin echo based techniques [4], the current method is more time efficient due to the use of multi-slab approach. For future development, optimization on diffusion directions and further reduction of total acquisition time per one 3D volume with parallel imaging can further reduce the sensitivity of 3D diffusion acquisition to motion yielding higher quality diffusion metrics maps.

References: [1] Jung et al, JMRI. 29: 1174-1184, 2009; [2] Zhang et al, ISMRM 2009, p. 168; [3] McNab et al, MRM, in press [4] Frank et al, Neuroimage, in press; [5] Van et al, IEEE TMI. 28: 1770-1780, 2009; [6] Van et al, ISMRM 2009, p. 1391; [7] Parker et al, MRM. 17: 434-451, 1991; [8] Nunes et al, JMR. 177: 102-110, 2005; [9] Fessler et al, IEEE Trans. Sig. Proc. 51: 560-574, 2003.

$$\frac{SNR_{3D}(\text{multi})}{SNR_{3D}(\text{single})} = \frac{1 - 2 \exp\left(-\frac{(RR \times n_{slab})/n_{exc} - TE/2}{T1}\right) + \exp\left(-\frac{(RR \times n_{slab})/n_{exc}}{T2}\right)}{1 - 2 \exp\left(-\frac{RR - TE/2}{T1}\right) + \exp\left(-\frac{RR}{T2}\right)} \times \sqrt{\frac{1}{n_{slab}}} \quad (1)$$

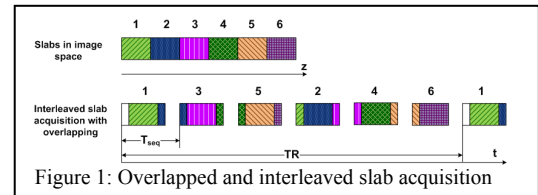


Figure 1: Overlapped and interleaved slab acquisition

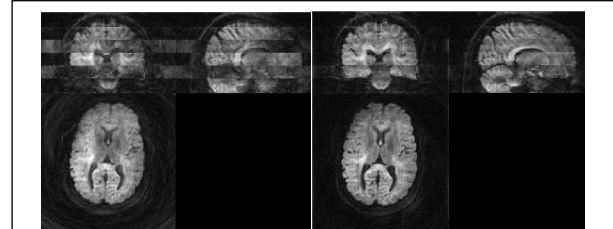


Figure 2: DW images: (a) without, (b) with phase error correction

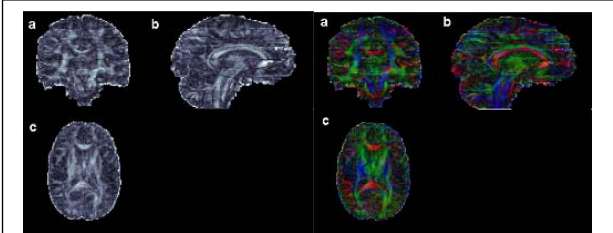


Figure 3: FA maps and color-coded FA maps